Universiteit Leiden
The Netherlands

Anomalous diffusion of Dirac fermions

Groth, C.W.

2 Electronic shot noise in fractal conductors

2.1 Introduction

Diffusion in a medium with a fractal dimension is characterized by an anomalous scaling with time t of the root-mean-squared displacement Δ. The usual scaling for integer dimensionality d is $\Delta \propto t^{1/2}$, independent of d. If the dimensionality d_f is noninteger, however, an anomalous scaling

$$\Delta \propto t^{1/(2+\alpha)} \tag{2.1}$$

with $\alpha > 0$ may appear. This anomaly was discovered in the early 1980's [144, 7, 21, 46, 109] and has since been studied extensively (see Refs. [53, 57] for reviews). Intuitively, the slowing down of the diffusion can be understood as arising from the presence of obstacles at all length scales – characteristic of a selfsimilar fractal geometry.

A celebrated application of the theory of fractal diffusion is to the scaling of electrical conduction in random-resistor networks (reviewed in Refs. [135, 111]). According to Ohm's law, the conductance G should scale with the linear size L of a d-dimensional network as $G \propto L^{d-2}$. In a fractal dimension the scaling is modified to $G \propto L^{d_f-2-\alpha}$, depending both on the fractal dimensionality d_f and on the anomalous diffusion exponent α. At the percolation threshold, the known [53] values for $d = 2$ are $d_f = 91/48$ and $\alpha = 0.87$, leading to a scaling $G \propto L^{-0.97}$. This almost inverse-linear scaling of the conductance of a planar random-resistor network

contrasts with the L-independent conductance $G \propto L^0$ predicted by Ohm's law in two dimensions.

All of this body of knowledge applies to classical resistors, with applications to disordered semiconductors and granular metals [128, 29]. The quantum Hall effect provides one quantum mechanical realization of a random-resistor network [140], in a rather special way because time-reversal symmetry is broken by the magnetic field. Recently [35], Cheianov, Fal'ko, Altshuler, and Aleiner announced an altogether different quantum realization in zero magnetic field. Following experimental [89] and theoretical [56] evidence for electron and hole puddles in undoped graphene[1], Cheianov et al. modeled this system by a degenerate electron gas[2] in a random-resistor network. They analyzed both the high-temperature classical resistance, as well as the low-temperature quantum corrections, using the anomalous scaling laws in a fractal geometry.

These recent experimental and theoretical developments open up new possibilities to study quantum mechanical aspects of fractal diffusion, both with respect to the Pauli exclusion principle and with respect to quantum interference (which are operative in distinct temperature regimes). To access the effect of the Pauli principle one needs to go beyond the time-averaged current $\bar{I}$ (studied by Cheianov et al. [35]), and consider the time-dependent fluctuations $\delta I(t)$ of the current in response to a time-independent applied voltage V. These fluctuations exist because of the granularity of the electron charge, hence their name "shot noise" (for reviews, see

[1] Graphene is a single layer of carbon atoms, forming a two-dimensional honeycomb lattice. Electrical conduction is provided by overlapping π-orbitals, with on average one electron per π-orbital in undoped graphene. Electron puddles have a little more than one electron per π-orbital (n-type doping), while hole puddles have a little less than one electron per π-orbital (p-type doping).

[2] An electron gas is called "degenerate" if the average occupation number of a quantum state is either close to unity or close to zero. It is called "nondegenerate" if the average occupation number is much smaller than unity for all states.

Refs. [24, 19]). Shot noise is quantified by the noise power

$$P = 2\int_{-\infty}^{\infty} dt\, \langle \delta I(0)\delta I(t)\rangle \tag{2.2}$$

and by the Fano factor $F = P/2e\bar{I}$. The Pauli principle enforces $F < 1$, meaning that the noise power is smaller than the Poisson value $2e\bar{I}$ – which is the expected value for independent particles (Poisson statistics).

The investigation of shot noise in a fractal conductor is particularly interesting in view of two different experimental results [41, 37] that have been reported. Both experiments measure the shot noise power in a graphene flake and find $F < 1$. A calculation [141] of the effect of the Pauli principle on the shot noise of undoped graphene predicted $F = 1/3$ in the absence of disorder, with a rapid suppression upon either p-type or n-type doping. This prediction is consistent with the experiment of Danneau et al. [37], but the experiment of DiCarlo et al. [41] gives instead an approximately *doping-independent* F near $1/3$. Computer simulations [118, 80] suggest that disorder in the samples of DiCarlo et al. might cause the difference.

Motivated by this specific example, we study here the fundamental problem of shot noise due to anomalous diffusion in a fractal conductor. While *equilibrium* thermal noise in a fractal has been studied previously [110, 51, 43], it remains unknown how anomalous diffusion might affect the *nonequilibrium* shot noise. Existing studies [77, 31, 68] of shot noise in a percolating network were in the regime where *inelastic* scattering dominates, leading to hopping conduction, while for diffusive conduction we need predominantly *elastic* scattering.

2.2 Results and discussion

We demonstrate that anomalous diffusion affects P and $\bar{I}$ in such a way that the Fano factor (their ratio) becomes scale independent as well as independent of d_f and α. Anomalous diffusion, therefore,

produces the same Fano factor $F = 1/3$ as is known [18, 96] for normal diffusion. This is a remarkable property of diffusive conduction, given that hopping conduction in a percolating network does not produce a scale-independent Fano factor [77, 31, 68]. Our general findings are consistent with the doping independence of the Fano factor in disordered graphene observed by DiCarlo et al. [41].

To arrive at these conclusions we work in the experimentally relevant regime where the temperature T is sufficiently high that the phase coherence length is $\ll L$, and sufficiently low that the inelastic length is $\gg L$. Quantum interference effects can then be neglected, as well as inelastic scattering events. The Pauli principle remains operative if the thermal energy kT remains well below the Fermi energy, so that the electron gas remains degenerate.

We first briefly consider the case that the anomalous diffusion on long length scales is preceded by normal diffusion on short length scales. This would apply, for example, to a percolating cluster of electron and hole puddles with a mean free path l which is short compared to the typical size a of a puddle. We can then rely on the fact that $F = 1/3$ for a conductor of any shape, provided that the normal diffusion equation holds locally [97, 136], to conclude that the transition to anomalous diffusion on long length scales must preserve the one-third Fano factor.

This simple argument cannot be applied to the more typical class of fractal conductors in which the normal diffusion equation does not hold on short length scales. As representative for this class, we consider fractal lattices of sites connected by tunnel barriers. The local tunneling dynamics then crosses over into global anomalous diffusion, without an intermediate regime of normal diffusion.

2.2.1 Sierpiński lattice

A classic example is the Sierpiński lattice [130] shown in Fig. 2.1 (inset). Each site is connected to four neighbors by bonds that represent the tunnel barriers, with equal tunnel rate Γ through each

barrier. The fractal dimension is $d_f = \log_2 3$ and the anomalous diffusion exponent is [53] $\alpha = \log_2(5/4)$. The Pauli exclusion principle can be incorporated as in Ref. [84], by demanding that each site is either empty or occupied by a single electron. Tunneling is therefore only allowed between an occupied site and an adjacent empty site. A current is passed through the lattice by connecting the lower left corner to a source (injecting electrons so that the site remains occupied) and the lower right corner to a drain (extracting electrons so that the site remains empty). The resulting stochastic sequence of current pulses is the "tunnel exclusion process" of Ref. [112].

The statistics of the current pulses can be obtained exactly (albeit not in closed form) by solving a master equation [12]. We have calculated the first two cumulants by extending to a two-dimensional lattice the one-dimensional calculation of Ref. [112]. To manage the added complexity of an extra dimension we found it convenient to use the Hamiltonian formulation of Ref. [119]. The hierarchy of linear equations that we need to solve in order to obtain $\bar{I}$ and P is derived in the appendix.

The results in Fig. 2.1 demonstrate, firstly, that the shot noise power P scales as a function of the size L of the lattice with the same exponent $d_f - 2 - \alpha = \log_2(3/5)$ as the conductance; and, secondly, that the Fano factor F approaches $1/3$ for large L. More precisely, see Fig. 2.2, we find that $F - 1/3 \propto L^{-1.5}$ scales to zero as a power law, with $F - 1/3 < 10^{-4}$ for our largest L.

2.2.2 Percolating network

Turning now to the application to graphene mentioned in the introduction, we have repeated the calculation of shot noise and Fano factor for the random-resistor network of electron and hole puddles introduced by Cheianov et al. [35]. The results, shown in Fig. 2.3, demonstrate that the shot noise power P scales with the same exponent $L^{-0.97}$ as the conductance G (solid lines in the lower panel), and that the Fano factor F approaches $1/3$ for

large networks (upper panel). This is a random, rather than a deterministic fractal, so there remains some statistical scatter in the data, but the deviation of F from $1/3$ for the largest lattices is still $< 10^{-3}$ (see the circular data points in Fig. 2.2).

2.3 Conclusion

In conclusion, we have found that the universality of the one-third Fano factor, previously established for normal diffusion [18, 96, 97, 136], extends to anomalous diffusion as well. This universality might have been expected with respect to the fractal dimension d_f (since the Fano factor is dimension independent), but we had not expected universality with respect to the anomalous diffusion exponent α. The experimental implication of the universality is that the Fano factor remains fixed at $1/3$ as one crosses the percolation threshold in a random-resistor network – thereby crossing over from anomalous diffusion to normal diffusion. This is consistent with the doping-independent Fano factor measured in a graphene flake by DiCarlo et al. [41].

Appendix 2.A Calculation of the Fano factor for the tunnel exclusion process on a two-dimensional network

Here we present the method we used to calculate the Fano factor for the tunnel exclusion process in the Sierpiński lattice and in the random-resistor network. We follow the master equation approach of Refs. [112, 12]. The two-dimensionality of our networks requires a more elaborate bookkeeping, which we manage by means of the Hamiltonian formalism of Ref. [119].

2.A.1 Counting statistics

We consider a network of N sites, each of which is either empty or singly occupied. Two sites are called adjacent if they are directly connected by at least one bond. A subset $\mathcal{S}$ of the N sites is connected to the source and a subset $\mathcal{D}$ is connected to the drain. Each of the 2^N possible states of the network is reached with a certain probability at time t. We store these probabilities in the 2^N-dimensional vector $|P(t)\rangle$. Its time evolution in the tunnel exclusion process is given by the master equation

$$\frac{d}{dt}|P(t)\rangle = M|P(t)\rangle\,, \tag{2.3}$$

where the matrix M contains the tunnel rates. The normalization condition can be written as $\langle\Sigma|P\rangle = 1$, in terms of a vector $\langle\Sigma|$ that has all 2^N components equal to 1. This vector is a left eigenstate of M with zero eigenvalue

$$\langle\Sigma|\,M = 0, \tag{2.4}$$

because every column of M must sum to zero in order to conserve probability. The right eigenstate with zero eigenvalue is the stationary distribution $|P_\infty\rangle$. All other eigenvalues of M have a real part < 0.

We store in the vector $|P(t,Q)\rangle$ the conditional probabilities that a state is reached at time t after precisely Q charges have entered the network from the source. Because the source remains occupied, a charge which has entered the network cannot return back to the source but must eventually leave through the drain. One can therefore use Q to represent the number of transfered charges. The time evolution of $|P(t,Q)\rangle$ reads

$$\frac{d}{dt}|P(t,Q)\rangle = M_0|P(t,Q)\rangle + M_1|P(t,Q-1)\rangle\,, \tag{2.5}$$

where $M = M_0 + M_1$ has been decomposed into a matrix M_0 containing all transitions by which Q does not change and a matrix M_1 containing all transitions that increase Q by 1.

The probability $\langle\Sigma|P(t,Q)\rangle$ that Q charges have been transferred through the network at time t represents the counting statistics. It describes the entire statistics of current fluctuations. The cumulants

$$C_n = \left.\frac{\partial^n S(t,\chi)}{\partial \chi^n}\right|_{\chi=0} \tag{2.6}$$

are obtained from the cumulant generating function

$$S(t,\chi) = \ln\left[\sum_Q \langle\Sigma|P(t,Q)\rangle\, \mathrm{e}^{\chi Q}\right]. \tag{2.7}$$

The average current and Fano factor are given by

$$\bar{I} = \lim_{t\to\infty} C_1/t, \quad F = \lim_{t\to\infty} C_2/C_1. \tag{2.8}$$

The cumulant generating function (2.7) can be expressed in terms of a Laplace transformed probability vector $|P(t,\chi)\rangle = \sum_Q |P(t,Q\rangle\, \mathrm{e}^{\chi Q}$ as

$$S(t,\chi) = \ln\langle\Sigma|P(t,\chi)\rangle\,. \tag{2.9}$$

Transformation of Eq. (2.5) gives

$$\frac{d}{dt}|P(t,\chi)\rangle = M(\chi)\,|P(t,\chi)\rangle\,, \tag{2.10}$$

where we have introduced the counting matrix

$$M(\chi) = M_0 + \mathrm{e}^{\chi} M_1. \tag{2.11}$$

The cumulant generating function follows from

$$S(t,\chi) = \ln\langle\Sigma|\,\mathrm{e}^{tM(\chi)}\,|P(0,\chi)\rangle\,. \tag{2.12}$$

The long-time limit of interest for the Fano factor can be implemented as follows [12]. Let $\mu(\chi)$ be the eigenvalue of $M(\chi)$ with the largest real part, and let $|P_\infty(\chi)\rangle$ be the corresponding (normalized) right eigenstate,

$$M(\chi)\,|P_\infty(\chi)\rangle = \mu(\chi)\,|P_\infty(\chi)\rangle\,, \tag{2.13}$$

$$\langle\Sigma|P_\infty(\chi)\rangle = 1. \tag{2.14}$$

Since the largest eigenvalue of $M(0)$ is zero, we have

$$M(0)\,|P_\infty(0)\rangle = 0 \Leftrightarrow \mu(0) = 0. \tag{2.15}$$

(Note that $|P_\infty(0)\rangle$ is the stationary distribution $|P_\infty\rangle$ introduced earlier.) In the limit $t \to \infty$ only the largest eigenvalue contributes to the cumulant generating function,

$$\lim_{t\to\infty} \frac{1}{t} S(t,\chi) = \lim_{t\to\infty} \frac{1}{t} \ln\left[e^{t\mu(\chi)}\,\langle\Sigma|P_\infty(\chi)\rangle\right] = \mu(\chi). \tag{2.16}$$

2.A.2 Construction of the counting matrix

The construction of the counting matrix $M(\chi)$ is simplified by expressing it in terms of raising and lowering operators, so that it resembles a Hamiltonian of quantum mechanical spins [119]. First, consider a single site with the basis states $|0\rangle = \binom{1}{0}$ (vacant) and $|1\rangle = \binom{0}{1}$ (occupied). We define, respectively, raising and lowering operators

$$s^+ = \begin{pmatrix} 0 & 0 \\ 1 & 0 \end{pmatrix}, \quad s^- = \begin{pmatrix} 0 & 1 \\ 0 & 0 \end{pmatrix}. \tag{2.17}$$

We also define the electron number operator $n = s^+ s^-$ and the hole number operator $\nu = \mathbb{1} - n$ (with $\mathbb{1}$ the 2×2 unit matrix). Each site i has such operators, denoted by s_i^+, s_i^-, n_i, and ν_i. The matrix $M(\chi)$ can be written in terms of these operators as

$$\begin{aligned} M(\chi) = &\sum_{\langle i,j\rangle} \left(s_j^+ s_i^- - \nu_j n_i\right) \\ &+ \sum_{i\in\mathcal{S}} (e^{\chi} s_i^+ - \nu_i) + \sum_{i\in\mathcal{D}} (s_i^- - n_i), \end{aligned} \tag{2.18}$$

where all tunnel rates have been set equal to unity. The first sum runs over all ordered pairs $\langle i,j\rangle$ of adjacent sites. These are Hermitian contributions to the counting matrix. The second sum runs over sites in $\mathcal{S}$ connected to the source, and the third sum runs over sites in $\mathcal{D}$ connected to the drain. These are non-Hermitian contributions.

It is easy to convince oneself that $M(0)$ is indeed M of Eq. (2.3), since every possible tunneling event corresponds to two terms in Eq. (2.18): one positive non-diagonal term responsible for probability gain for the new state and one negative diagonal term responsible for probability loss for the old state. In accordance with Eq. (2.11), the full $M(\chi)$ differs from M by a factor e^{χ} at the terms associated with charges entering the network.

2.A.3 Extraction of the cumulants

In view of Eq. (2.16), the entire counting statistics in the long-time limit is determined by the largest eigenvalue $\mu(\chi)$ of the operator (2.18). However, direct calculation of that eigenvalue is feasible only for very small networks. Our approach, following Ref. [112], is to derive the first two cumulants by solving a hierarchy of linear equations.

We define

$$T_i = \langle\Sigma|\, n_i \,|P_\infty(\chi)\rangle = 1 - \langle\Sigma|\, \nu_i \,|P_\infty(\chi)\rangle\,, \tag{2.19}$$

$$U_{ij} = U_{ji} = \langle\Sigma|\, n_i n_j \,|P_\infty(\chi)\rangle \quad \text{for } i \neq j, \tag{2.20}$$

$$U_{ii} = 2T_i - 1. \tag{2.21}$$

The value $T_i|_{\chi=0}$ is the average stationary occupancy of site i. Similarly, $U_{ij}|_{\chi=0}$ for $i \neq j$ is the two-point correlator.

We will now express $\mu(\chi)$ in terms of T_i. We start from the definition (2.13). If we act with $\langle\Sigma|$ on the left-hand-side of Eq. (2.13) we obtain

$$\begin{aligned}
&\langle\Sigma|\, M(0) + (e^{\chi}-1)\sum_{i\in\mathcal{S}} s_i^+ \,|P_\infty(\chi)\rangle \\
&\qquad = (e^{\chi}-1)\sum_{i\in\mathcal{S}} \langle\Sigma|\, s_i^+ \,|P_\infty(\chi)\rangle \\
&\qquad = (e^{\chi}-1)\sum_{i\in\mathcal{S}} \langle\Sigma|\, \nu_i \,|P_\infty(\chi)\rangle \\
&\qquad = (e^{\chi}-1)\sum_{i\in\mathcal{S}} (1-T_i).
\end{aligned} \tag{2.22}$$

In the second equality we have used Eq. (2.4) [which holds since $M \equiv M(0)$]. Acting with $\langle\Sigma|$ on the the right-hand-side of Eq. (2.13) we obtain just $\mu(\chi)$, in view of Eq. (2.14). Hence we arrive at

$$\mu(\chi) = (\mathrm{e}^{\chi} - 1) \sum_{i \in \mathcal{S}} (1 - T_i). \tag{2.23}$$

From Eq. (2.23) we obtain the average current and Fano factor in terms of T_i and the first derivative $T_i' = dT_i/d\chi$ at $\chi = 0$,

$$\bar{I} = \lim_{t\to\infty} C_1/t = \mu'(0) = \sum_{i \in \mathcal{S}} (1 - T_i|_{\chi=0}), \tag{2.24}$$

$$F = \lim_{t\to\infty} \frac{C_2}{C_1} = \frac{\mu''(0)}{\mu'(0)} = 1 - \frac{2\sum_{i\in\mathcal{S}} T_i'|_{\chi=0}}{\sum_{i\in\mathcal{S}}(1 - T_i|_{\chi=0})}. \tag{2.25}$$

Average current

To obtain T_i we set up a system of linear equations starting from

$$\mu(\chi) T_i = \langle\Sigma|\, n_i M(\chi)\, |P_\infty(\chi)\rangle\,. \tag{2.26}$$

Commuting n_i to the right, using the commutation relations $[n_i, s_i^+] = s_i^+$ and $[n_i, s_i^-] = -s_i^-$, we find

$$\mu(\chi) T_i = \sum_{j(i)} T_j - k_i T_i + k_{i,\mathcal{S}} + (\mathrm{e}^{\chi} - 1) \sum_{l \in \mathcal{S}} (T_i - U_{li}). \tag{2.27}$$

The notation $\sum_{j(i)}$ means that the sum runs over all sites j adjacent to i. The number k_i is the total number of bonds connected to site i; $k_{i,\mathcal{S}}$ of these bonds connect site i to the source.

In order to compute $T_i|_{\chi=0}$ we set $\chi = 0$ in Eq. (2.27), use Eq. (2.15) to set the left-hand-side to zero, and solve the resulting symmetric sparse linear system of equations,

$$-k_{i,\mathcal{S}} = \sum_{j(i)} T_j - k_i T_i. \tag{2.28}$$

This is the first level of the hierarchy. Substitution of the solution into Eq. (2.24) gives the average current $\bar{I}$.

Fano factor

To calculate the Fano factor via Eq. (2.25) we also need $T_i'|_{\chi=0}$. We take Eq. (2.27), substitute Eq. (2.23) for $\mu(\chi)$, differentiate and set $\chi = 0$ to arrive at

$$\sum_{l\in\mathcal{S}}(U_{li} - T_l T_i) - k_{i,\mathcal{S}} = \sum_{j(i)} T_j' - k_i T_i'. \tag{2.29}$$

To find $U_{ij}|_{\chi=0}$ we note that

$$\mu(\chi)U_{ij} = \langle\Sigma|\, n_i n_j M(\chi)\,|P_\infty(\chi)\rangle\,, \quad i \neq j, \tag{2.30}$$

and commute n_i to the right. Setting $\chi = 0$ provides the second level of the hierarchy of linear equations,

$$\begin{aligned} 0 = &\sum_{l(j),l\neq i} U_{il} + \sum_{l(i),l\neq j} U_{jl} - (k_i + k_j - 2d_{ij})U_{ij} \\ &+ k_{j,\mathcal{S}} T_i + k_{i,\mathcal{S}} T_j, \quad i \neq j. \end{aligned} \tag{2.31}$$

The number d_{ij} is the number of bonds connecting sites i and j if they are adjacent, while $d_{ij} = 0$ if they are not adjacent.

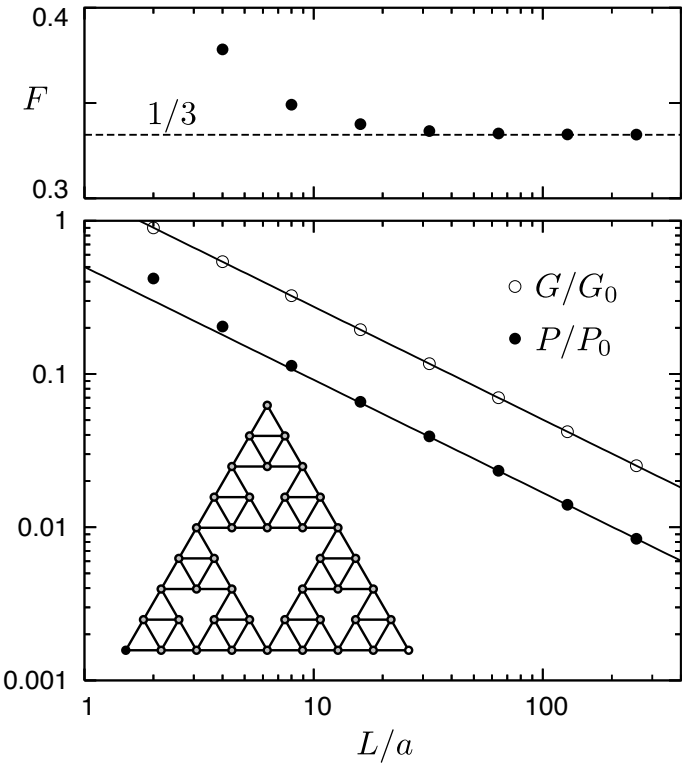

Figure 2.1: Lower panel: Electrical conduction through a Sierpiński lattice. This is a deterministic fractal, constructed by recursively removing a central triangular region from an equilateral triangle. The recursion level r quantifies the size $L = 2^r a$ of the fractal in units of the elementary bond length a (the inset shows the fourth recursion). The conductance $G = \bar{I}/V$ (open dots, normalized by the tunneling conductance G_0 of a single bond) and shot noise power P (filled dots, normalized by $P_0 = 2eVG_0$) are calculated for a voltage difference V between the lower-left and lower-right corners of the lattice. Both quantities scale as $L^{d_f-2-\alpha} = L^{\log_2(3/5)}$ (solid lines on the double-logarithmic plot). The Fano factor $F = P/2e\bar{I} = (P/P_0)(G_0/G)$ rapidly approaches 1/3, as shown in the upper panel.

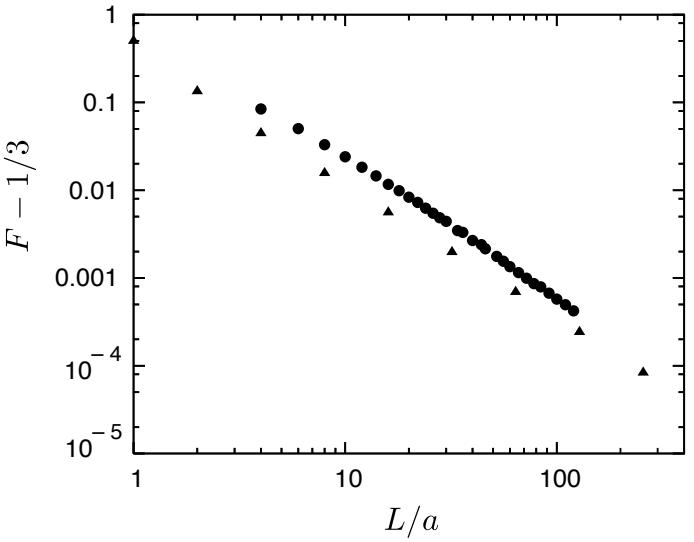

Figure 2.2: The deviation of the Fano factor from $1/3$ scales to zero as a power law for the Sierpiński lattice (triangles) and for the random-resistor network (circles).

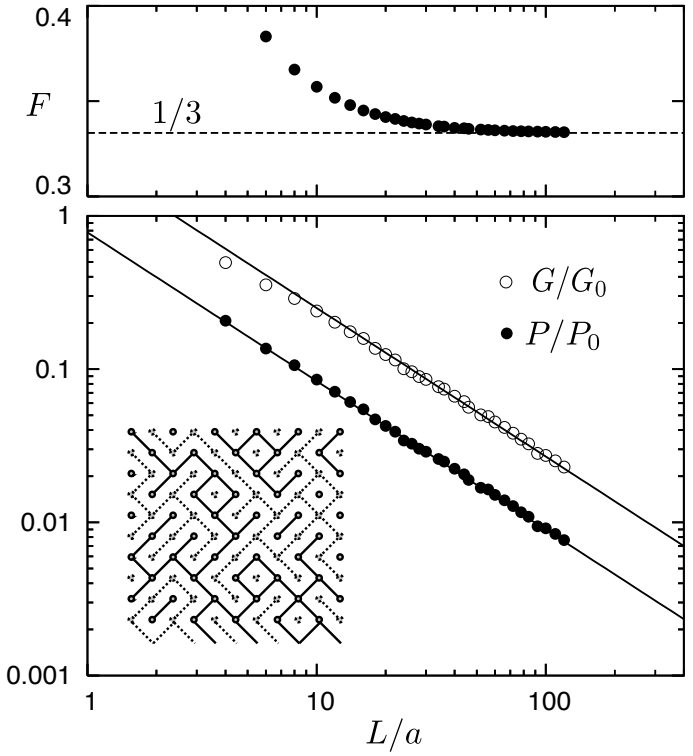

Figure 2.3: Same as Fig. 2.1, but now for the random-resistor network of disordered graphene introduced by Cheianov et al. [35]. The inset shows one realization of the network for $L/a = 10$ (the data points are averaged over $\simeq 10^3$ such realizations). The alternating solid and dashed lattice sites represent, respectively, the electron (n) and hole (p) puddles. Horizontal bonds (not drawn) are p-n junctions, with a negligibly small conductance $G_{pn} \approx 0$. Diagonal bonds (solid and dashed lines) each have the same tunnel conductance G_0. Current flows from the left edge of the square network to the right edge, while the upper and lower edges are connected by periodic boundary conditions. This plot is for undoped graphene, corresponding to an equal fraction of solid (n-n) and dashed (p-p) bonds.